INVERSE ESTIMATION OF SOIL HYDRAULIC AND SOLUTE TRANSPORT PARAMETERS FROM TRANSIENT FIELD EXPERIMENTS: HETEROGENEOUS SOIL

F. Abbasi, D. Jacques, J. Simunek, J. Feyen, M. Th. van Genuchten

ABSTRACT. *While inverse parameter estimation techniques for determining key parameters affecting water flow and solute transport are becoming increasingly common in saturated and unsaturated zone studies, their application to practical problems, such as irrigation, have received relatively little attention. In this article, we used the Levenberg–Marquardt optimization algorithm in combination with the HYDRUS–2D numerical code to estimate soil hydraulic and solute transport parameters of several soil horizons below experimental furrows. Three experiments were carried out, each of the same duration but with different amounts of water and solutes resulting from 6, 10, and 14 cm water depths in the furrows. Two more experiments were performed with the same amounts of applied water and solute and, consequently, for different durations, on furrows with depths of 6 and 10 cm of water. We first used a scaling method to characterize spatial variability in the soil hydraulic properties, and then simultaneously estimated the saturated hydraulic conductivity (K_s) and the longitudinal dispersivity (D_L) for the different horizons. Model predictions showed only minor improvements over those previously obtained assuming homogeneous soil profiles. In an effort to improve the predictions, we also carried out a two–step, sequential optimization in which we first estimated the soil hydraulic parameters followed by estimation of the solute transport parameters. This approach allowed us to include additional parameters in the optimization process. A sensitivity analysis was performed to determine the most sensitive hydraulic and solute transport parameters. Soil water contents were found to be most sensitive to the n parameter in van Genuchten's soil hydraulic model, followed by the saturated water content (θ_s), while solute concentrations were most affected by θ_s and D_L. For these reasons, we estimated θ_s and n for the various soil horizons of the sequential optimization process during the first step, and only D_L during the second step. Sequential estimation somewhat improved predictions of the cumulative infiltration rates during the first irrigation event. It also significantly improved descriptions of the soil water content, particularly of the upper horizons, as compared to those obtained using simultaneous estimation, whereas deep percolation rates of water did not improve. Solute concentrations in the soil profiles were predicted equally well with both optimization approaches.*

Keywords. *Furrow irrigation, Heterogeneous soil, Inverse solution, Scaling, Solute transport, Water flow.*

Understanding solute transport processes between the soil surface and the groundwater table is essential for limiting or effectively managing soil and groundwater pollution. Unfortunately, solute transport, particularly at the field scale under transient conditions, can be very complex because of the presence of several mutually interactive soil physical, chemical, and biological processes that may vary substantially over space and time. Previous studies have shown that water flow and solute transport processes are influenced by soil type (Vanderborght et al., 1997, 2001), flow rate (Vanderborght et al., 1997; Forrer et al., 1999; Wildenschild et al., 2001), flow regime (Bowman and Rice, 1986; Jaynes et al., 1988), irrigation method (Ghodrati and Jury, 1990; Troiano et al., 1993; Flury et al., 1994), surface flow depth (Abbasi et al., 2003a), preferential flow (Flury et al., 1994; van Weesenbeeck and Kachanoski, 1994), soil heterogeneity (Roth et al., 1991; Jacques, 2000), initial conditions (White et al., 1986; Steenhuis and Muck, 1988), and/or boundary conditions (Russo et al., 1994a, 1994b).

Some field studies suggest that solute transport in heterogeneous soils can be described with the classical convection–dispersion equation (CDE) (e.g. Roth et al., 1991; Butters and Jury, 1989), while others show considerable deviations between model predictions and field data (e.g. Snow et al., 1994; de Vos, 1997; Jacques et al., 1998). Roth at al. (1991) found that the CDE model described their tracer data well for transport distances less than 1 m, whereas the findings of Butters and Jury (1989) showed good correspondence only after a travel distance of 4 m. Several commonly observed features of solute transport, such as multiple peak breakthrough curves and fingered flow, cannot be described with the CDE model. Ventrella et al. (2000) and Jacques et al. (2002) found that the mobile–immobile (MIM) approach described observed breakthrough curves (BTC)

Article was submitted for review in July 2002; approved for publication by the Soil & Water Division of ASAE in May 2003.

The authors are **Fariborz Abbasi,** Soil Physicist, and **Jan Feyen,** Professor, Institute for Land and Water Management, Katholieke Universiteit Leuven, Belgium; **Deiderik Jacques,** Soil Physicist, Waste and Disposal Department, SCK–CEN, Mol, Belgium; and **Jirka Simunek,** Soil Physicist, and **Martinus Th. van Genuchten,** Research Leader, USDA–ARS, George E. Brown Jr. Salinity Laboratory, Riverside, California. **Corresponding author:** Jan Feyen, Institute for Land and Water Management, Vital Decosterstraat 102, 3000–Leuven, Belgium; phone: +32–16–329756; fax: +32–16–329760; e–mail: jan.feyen@agr.kuleuven.ac.be.

better than the CDE model for chloride transport in heterogeneous soils under natural boundary conditions. By contrast, Jacques et al. (1998, 2002) and Snow et al. (1994), among others, found that the CDE and MIM models both underestimated the rate of transport (early breakthrough) of their observed data.

Identification and accurate simulation of field–scale water flow and solute transport processes, especially when subject to natural boundary conditions, is a complex task since many input parameters are difficult to measure at the desired scale, while their temporal and spatial variability often cannot be easily described. However, combining numerical solutions of the governing flow and transport equations with inverse optimization algorithms and detailed measurement of different variables is a promising approach for process and parameter identification (Jacques et al., 2002). A common way to estimate flow and transport parameters is by using inverse optimization techniques whereby differences between measured and model–predicted values are minimized. Inverse methods are increasingly being used to estimate soil hydraulic parameters (e.g., Gribb, 1996; Simunek and van Genuchten, 1996, 1997; Kodesova et al., 1998, 1999; Simunek et al., 2001; among others), or in combination with solute transport or root water uptake parameters (Ventrella et al., 2000; Inoue et al., 2000; Wildenschild et al., 2001; Vrugt et al., 2001; Jacques et al., 2002; Simunek et al., 2002). In spite of considerable efforts in estimating soil hydraulic and transport properties by means of inverse modeling, their application to practical problems, particularly irrigation, has received a little attention.

Abbasi et al. (2003b) recently applied inverse methods to several 2–D furrow irrigation experiments assuming homogeneous soil profiles, and simultaneously estimated the saturated hydraulic conductivity (K_s) and several solute transport parameters. For solute transport, they used both the equilibrium (CDE) and nonequilibrium (MIM) transport models. In this study, we revisit the analysis by Abbasi et al. (2003b) assuming a layered profile and also consider sequential estimation. Since the MIM model did not lead to significant improvements in the model predictions for the homogeneous case (Abbasi et al., 2003b), we limit ourselves in this study to only the equilibrium transport model. Hence, the purpose of this article is to use simultaneous and sequential optimization to estimate the soil hydraulic and solute transport parameters for different soil horizons from several furrow flow and transport experiments. A scaling method will be used to characterize spatial variability in the soil hydraulic properties. Simulations and inverse analyses will be carried out using the HYDRUS–2D variably saturated flow/transport code of Simunek et al. (1999), which includes the Levenberg–Marquardt parameter optimization algorithm. Model predictions will be compared with field–measured cumulative infiltration rates, soil water contents, bromide concentrations, and both water and solute deep percolation rates.

Materials and Methods

Field Experiments

Field experiments were conducted at the Maricopa Agricultural Center (MAC) in Phoenix, Arizona, on a bare Casa Grande sandy loam soil on short blocked–end furrows. Five soil horizons were identified in the experimental area: a 33 cm thick surface Ap horizon, followed by a Btkn1 horizon between 33 and 58 cm having a calcium carbonate content that increased with depth, a Btkn2 horizon between 58 and 71 cm, a Btkn3 horizon between 71 and 125 cm, and a 2Bkn horizon between 125 and 152 cm.

Two series of experiments were carried out. We first performed same–duration (SD) experiments that involved three flow depths (6, 10, and 14 cm), each with two irrigations, 10 days apart. The first irrigation took place in two phases. During the first phase, water was applied for 60 min (the same for all three experiments) to wet the soil profile. During the second phase, water amended with $CaBr_2$ was applied for 30 min, again the same for the three plots. The second irrigation lasted 90 min using the same depths of unamended water as for the first irrigation.

The second series of experiments involved similar amounts of applied water and solutes (SWS). The amount of applied water was the same as that infiltrated for the 14 cm depth treatment of the SD experiments. Water levels of 6 and 10 cm were used in this case. The first irrigation was again carried out in two steps, similarly as for the SD scenarios, with unamended water being applied first followed by bromide–amended water. However, the irrigation times were adjusted for each of the water levels such that predefined amounts of water infiltrated (i.e., the amount given during the previous 14 cm SD experiment). The second irrigation used unamended water applied with the same water levels as for the first irrigation, but with times adjusted so that again the same amount of water infiltrated during the second irrigation as for the 14 cm depth treatment in the first set of SD experiments.

A set of five neutron probe access tubes (each 3.3 m in depth) was installed to measure soil water contents at different locations perpendicular to the axis of the monitored furrows. Readings were taken at depths of 20, 40, 60, 80, 100, 140, 180, 220, and 260 cm before each irrigation to provide initial conditions, immediately after each irrigation, then hourly up to 6 hours after each irrigation, and subsequently each 3 hours up to 24 hours. Measurements were later taken 3 to 4 times per day up to 3 days after irrigation, and then 1 to 2 times per day up to the next irrigation. Water contents of the surface layer (0 to 30 cm) were also measured using a site–calibrated time domain reflectometry (TDR) probe. The TDR and neutron probe readings were taken at the same times as indicated above.

Soil samples for analyzing bromide concentrations were taken manually, at depths (up to 180 cm) and locations corresponding to the neutron probe access tube measurements, four times during the experiments, i.e., prior to the experiments as initial values, 5 days after the first irrigation, and 6 and 20 days after the second irrigation. Soil extractions (1:1 weight:volume) were made and analyzed for bromide with a Lachat QuikChem flow injection analyzer using standard colorimetric procedures.

The SD and SWS experiments started on 30 January and 26 February 2001, respectively, and each lasted 30 days. Further information about the experiments can be found in Abbasi et al. (2003a, 2003b).

Governing Water Flow and Solute Transport Equations

The Richards equation (Richards, 1931) describing two–dimensional isothermal Darcian water flow in a variably saturated rigid porous medium and the physical equilibrium convection–dispersion equation (CDE) were used as the governing equations for water flow and solute transport, respectively. The CDE equation was previously found to be suitable for this soil (Abbasi et al., 2003b). No significant improvements in predictions of calculated concentrations were obtained when the physical nonequilibrium MIM model was used. Calculations based on the governing flow and transport equations were carried out using the HYDRUS–2D code (Simunek et al., 1999), and the minimization problem for parameter optimization was carried out using the Levenberg–Marquardt nonlinear weighted least–squares approach (Marquardt, 1963) as implemented in HYDRUS–2D.

Measured bromide concentrations and soil water contents before the experiments were used as initial conditions within the soil profile below the furrows. A constant pressure head (surface ponding) was specified as the upper boundary condition in the furrow during irrigation, while an atmospheric boundary condition was used after irrigation during the redistribution phase. A Cauchy condition was used for the upper boundary condition for solute transport, and free–drainage conditions for both water and solute were used at the lower boundary of the domain. No–flux boundary conditions were applied to both sides of the flow domain. The furrows were 100 cm wide, while the soil profile was assumed to be 100 cm deep in our simulations.

Characterization of the Soil Hydraulic Properties

Spatial variability in the soil hydraulic properties remains one of the major problems in field–scale analyses of water flow and solute transport. One way of characterizing this spatial variability is by scaling locally measured soil water retention and hydraulic conductivity data to reference curves using scaling factors (Hopmans, 1989; Vogel et al., 1991; Eching et al., 1994). This concept is known as functional similarity (Simmons et al., 1979). In this article, laboratory–measured soil water retention curves (no hydraulic conductivity measurements were made) for the different horizons were scaled using linear scaling relationships proposed by Vogel et al. (1991). Neglecting time variability in the soil hydraulic properties, the scaling factors and their relationships to the reference curves are as follows (Vogel et al., 1991):

$$\theta(x,h)=\theta_r(x)+\alpha_\theta(x)[\theta^*(h^*)-\theta_r^*] \tag{1}$$

$$h=\alpha_h(x)h^* \tag{2}$$

where

- θ = water content ($L^3\ L^{-3}$)
- h = pressure head (L)
- $\theta^*(h^*)$ = reference retention curve
- θ_r = residual soil water contents ($L^3\ L^{-3}$) of the local retention curves
- θ^*_r = residual soil water contents ($L^3\ L^{-3}$) of the reference retention curves
- x = vector of spatial coordinates
- α_θ = scaling factors for water contents
- α_h = scaling factors for pressure heads.

The reference soil water retention curve, $\theta^*(h^*)$, is described using the closed–form equation of van Genuchten (1980):

$$\theta^*(h^*)=\theta_r^*+\frac{\theta_s^*-\theta_r^*}{(1+|\alpha h^*|^n)^m} \tag{3}$$

and the unsaturated soil hydraulic conductivity function, $K(h^*)$, using the pore–size distribution model of Mualem (1976), as follows (van Genuchten, 1980):

$$K(h^*) = K_s S_e^{\,l}\,[1-(1-S_e^{1/m})^m]^2 \tag{4}$$

where

$$S_e=\frac{\theta^*-\theta_r^*}{\theta_s^*-\theta_r^*},\quad m=1-\frac{1}{n},\quad n>1 \tag{5}$$

and

- θ^*_s = saturated water content ($L^3\ L^{-3}$)
- S_e = relative saturation (dimensionless)
- m, n, l, α = empirical parameters (m, n, and l dimension–less; α in L^{-1}).

The parameters of the reference water retention curve and the scaling factors α_θ and α_h were determined by minimizing the squared differences between the reference water contents and scaled measured water contents, subject to the constraint that the average of α_θ and α_h be unity (e.g., Warrick et al., 1977; Vogel et al., 1991; Jacques, 2000). In this study, θ^*_s and θ^*_r were fixed at the average of the fitted local θ_r and θ_s values, respectively, while l in equation 4 was assumed to be 0.5 (Mualem, 1976). Undisturbed soil samples (6 cm long and 5.4 cm diameter) were collected from different soil horizons up to a depth of 100 cm to estimate parameters in the van Genuchten (VG) soil hydraulic model. The scaling analysis was carried out separately for each of the soil horizons.

Sensitivity Analysis

Prior to analyzing the actual field data, a sensitivity analysis was performed to determine the most sensitive soil hydraulic and solute transport parameters. The sensitivity of the measured variables to various model parameters was evaluated using sensitivity coefficients. Sensitivity coefficients, $s(z,t,b_j)$, were determined according to Simunek et al. (1998) as follows:

$$s(z,t,b_j)=|Y(b+\Delta b e_j)-Y(b)| \tag{6}$$

where

- $s(z,t,b_j)$ = change in variable Y (the soil water content or the solute concentration) corresponding to a 1% change in parameter b_j
- e_j = jth unit vector
- Δb = 0.01b.

Sensitivity coefficients were multiplied by 100 in equation 6 to avoid very small numerical values.

The sensitivity analysis was performed only for plot 3 assuming experimental conditions that were between the SD and SWS experiments, and for a duration of up to 10 days after the first irrigation event. We assumed 60 min irrigation with tap water, followed by a 30 min solute pulse application, as done during the field experiments. We evaluated sensitivi–

Table 1. Reference van Genuchten soil water retention parameters for the different soil horizons.

Soil Horizon	Depth (m)	θ_r ($cm^3\ cm^{-3}$)	θ_s ($cm^3\ cm^{-3}$)	α (cm^{-1})	n (–)
Ap	0–0.33	0.104	0.374	0.035	1.611
Btkn1	0.33–0.58	0.111	0.444	0.063	1.539
Btkn2	0.58–0.71	0.107	0.420	0.040	1.555
Btkn3	0.71–1.25[a]	0.103	0.412	0.047	1.554
CV (%)	—	2.93	6.10	22.9	1.75

[a] Soil samples were collected at a depth of 0.8.

ties of the soil water contents and solute concentrations to all retention parameters (assuming their scaled values as given in table 1), the saturated hydraulic conductivity (K_s), and the longitudinal (D_L) and transverse (D_T) dispersivities in the CDE transport model. Estimated values from our previous study (Abbasi et al., 2003b) were used for D_L, D_T, and K_s, while the exponent l in Mualem's expression was taken to be 0.5 during the sensitivity analysis.

Selection of Parameters for Optimization

The main objective of this study was to estimate soil hydraulic and solute transport parameters of the different soil horizons using two different optimization approaches. We tried to limit the number of unknown parameters for the following reasons: (1) uncertainty is generally reduced and non–physical parameter values are more likely avoided when a limited number of parameters is used in optimization studies (e.g., Simunek et al., 2001); (2) data showed only minor changes in water contents and solute concentrations below a depth of 100 cm, particularly for the same duration (SD) experiments (Abbasi et al., 2003a); (3) the majority of measurements were made in the upper 100 cm of the soil profiles, and only a limited number of measurements were made at deeper depths, thus providing insufficient information to optimize parameters for the lower horizons; and (4) simulation times needed to run the inverse option of HYDRUS–2D for our problem were considerable. Optimization of a complete set of parameters for our experiments took several days using a Pentium III PC.

For the simultaneous parameter estimation approach, twelve additional parameters must be optimized for the first four identified soil horizons (four values each of K_s, D_L, and D_T) when assuming that the retention properties are fully characterized by the reference scaling curves. For the reasons stated above, we limited the number of optimized parameters to less than ten. Previous optimization results assuming homogeneous soil profiles indicated low confidence in the optimized D_T values (broad confidence intervals). This parameter was also the least sensitive parameter among all soil hydraulic and solute transport parameters in our sensitivity analysis (see results below). For these reasons, we did not include D_T in the optimization process, but rather fixed it at values obtained for the homogeneous profiles. The remaining two parameters (K_s and D_L) were considered to be the most important and hence were optimized for each soil horizon separately (eight parameters in total). Among the soil hydraulic parameters, only K_s was optimized for the different soil horizons since we did not have direct measurement for K_s. Other soil hydraulic parameters during optimization were fixed for each soil horizon at the values given in table 1.

As will be discussed in the following sections, simultaneous estimation of the K_s and D_L parameters for the different horizons produced only minor improvements in the model predictions as compared to results obtained from our previous analysis assuming homogeneous soil profiles. We wanted to know if including additional soil hydraulic parameters would improve the predictions. However, as discussed above, it is not recommended to estimate too many parameters simultaneously due to instability of the inverse optimization methods. To overcome this problem, we also used sequential estimation, in which the soil hydraulic parameters are estimated first, followed by estimation of the solute transport parameters. In our study, we used two sequential steps. During the first step, the saturated soil water content (θ_s) and the n parameter in the VG soil hydraulic model, which were found to be the most sensitive parameters in our sensitivity analysis (discussed below), were optimized for the different soil horizons. During the second step, only D_L values were estimated. We did not include D_T in the second step since this often caused instability in the optimizations, with the model not converging to a unique solution for some experiments.

As indicated earlier, the optimization process was carried out using the Levenberg–Marquardt optimization algorithm (Marquardt, 1963), leading to minimization of an objective function, as discussed in detail by Abbasi et al. (2003b).

Results and Discussion

Scaling of Retention Properties

Measured (unscaled) and scaled soil water retention curves for the various soil horizons are shown in figure 1. Parameters of the reference curves and their coefficients of variations (CV) are given in table 1. The effect of scaling on the retention curves was more noticeable for the first and second soil horizons since more soil samples had been collected from these two horizons, thus revealing more spatial variability. The θ_r and n values remained almost constant with depth and showed relatively low CVs, while the α parameter exhibited much more variability, with a CV of 22.9%. Notice that θ_s for the first horizon was somewhat lower than for the other horizons. The CVs for n and α before scaling were 7% and 50%, respectively. These results agree well with findings of Mallants et al. (1996a), who also found more variability in α as compared to n.

Sensitivity Analyses

The sensitivities of the soil water contents and solute concentrations to soil hydraulic and transport parameters are given in figures 2a and 2b, respectively. Results are only shown for the vertical below the bottom of the furrow down to a depth of 100 cm since most changes generally occur in this region (note that the furrow depth was approximately 20 cm). Overall, water contents (fig. 2a) in the soil profile showed the highest sensitivity near the moisture front as it gradually moved to deeper depths with time. However, some sensitivity was also observed near the soil surface during the drier conditions starting about 8 days after water application. The largest sensitivity coefficients were observed in the lower part of the soil profile about 10 days after the irrigation. The most sensitive parameter was n, having a maximum sensitivity coefficient of 1.5, followed by θ_s. The exponent

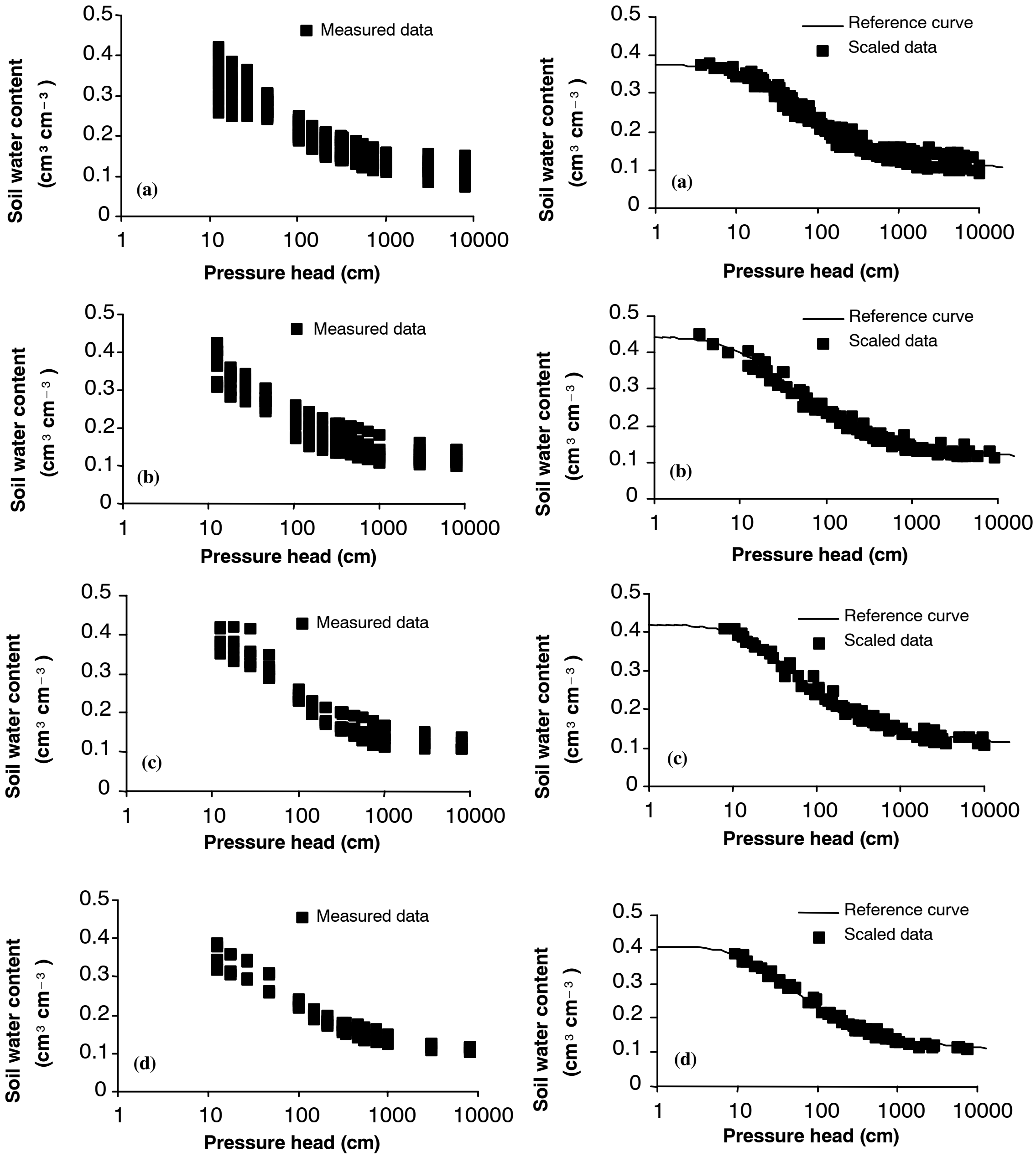

Figure 1. Measured (unscaled), scaled, and reference (fitted) soil water retention curves for the different soil horizons: (a) 0 to 0.33 m, (b) 0.33 to 0.58 m, (c) 0.58 to 0.71 m, and (d) 0.71 to 1.25 m.

l in the capillary model of Mualem (1976) was the least sensitive parameter. Contrary to the water contents, solute concentration sensitivities were more pronounced near the soil surface and gradually increased with time as the soil surface dried out (fig. 2b). The saturated water content (θ_s) was the most sensitive parameter, followed by the saturated hydraulic conductivity (K_s). The longitudinal dispersivity (D_L) appeared to be much more sensitive than the transverse dispersivity (D_T). This was not consistent with findings by Forrer et al. (1999), who found that D_T was more sensitive than D_L. Note that white zones in the different subplots of figure 2 are representative of small but non–zero values.

Parameter Optimization

Simultaneous Optimization

Simultaneously optimized K_s and D_L values for the various soil horizons and experimental plots are summarized in table 2. Corresponding values obtained from analyses assuming homogeneous soil profiles (Abbasi et al., 2003b) are also included in table 2 for comparison. The K_s values for the first horizon for the different experiments corresponded well with the optimized values for an equivalent homogeneous soil profile and those predicted with pedotransfer functions for a sandy loam soil (Schaap and Leij, 1998). The K_s values for the other horizons were slightly higher than for the first horizon (except for plot 1) and somewhat larger than those reported by Schaap and Leij (1998). However, they were consistent with those given by Carsel and Parrish (1988)

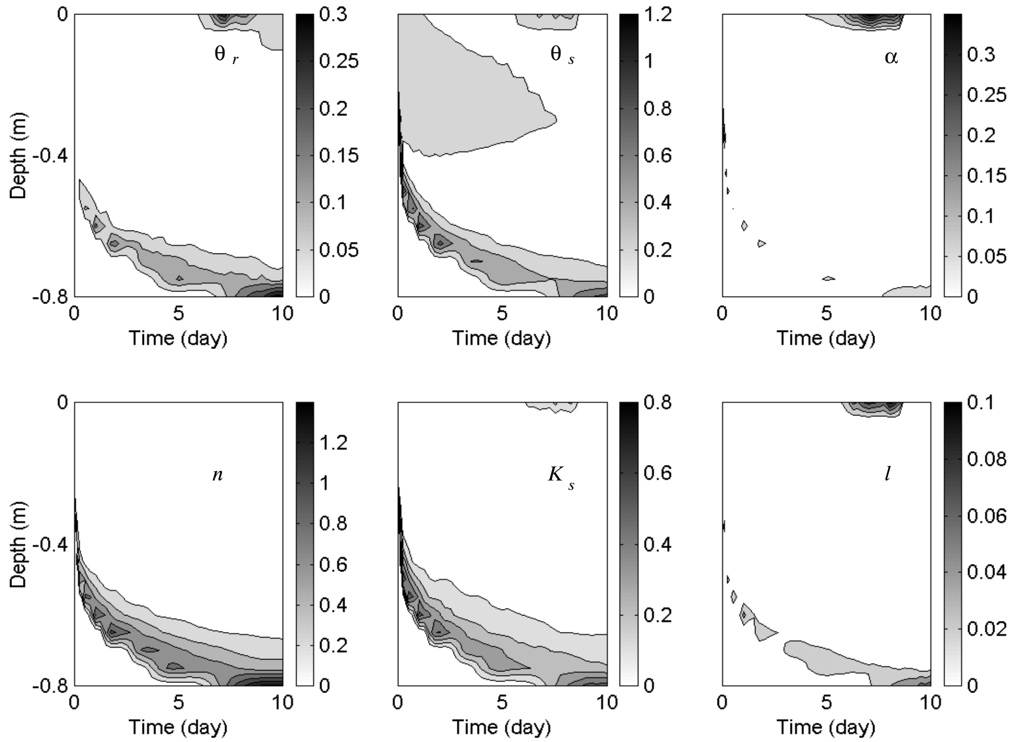

Figure 2a. Soil water content sensitivities to different soil hydraulic parameters as evaluated for plot 3, plotted along a vertical from the bottom of the furrow (20 cm below the soil surface) to a depth of 100 cm.

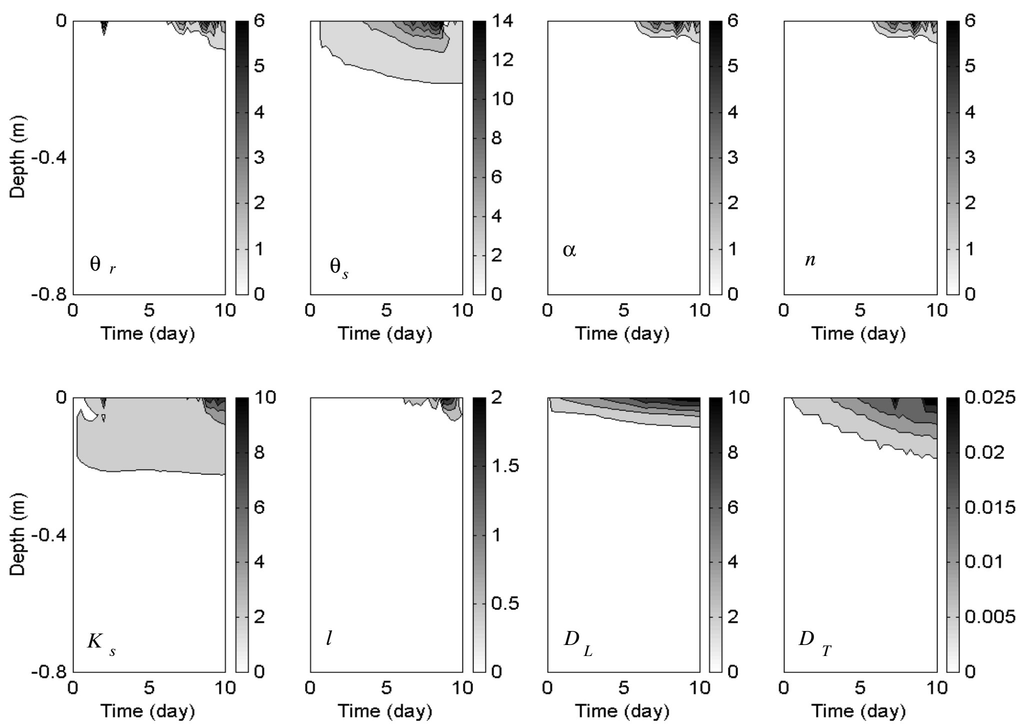

Figure 2b. Solute concentration sensitivities to different soil hydraulic and solute transport parameters as evaluated for plot 3, plotted along a vertical from the bottom of the furrow (20 cm below the soil surface) to a depth of 100 cm.

for corresponding soil textures. We believe that, rather than the deeper horizons having inherently higher saturated conductivities, the higher estimated K_s values of these horizons were more likely due to having fewer data from these depths. The K_s values of the upper horizons should be relatively well defined since they were estimated from the measured infiltration rates and measured soil water contents. However, the infiltration rate at the soil surface should not help much in estimating K_s for the deeper layers, for which the measured water content is the main information. Having soil water pressure head measurements probably would have helped to improve the estimation of K_s for the lower horizons.

Table 2. Summary of the simultaneously optimized saturated hydraulic conductivity (K_s) and longitudinal dispersivity (D_L) parameters for the different soil horizons and experimental plots. Corresponding parameters for analyses assuming homogeneous soil profiles are given in parentheses. Also included are values of the minimized objective function (SSQ) and the R^2 values of the optimizations.

Depth (m)	K_s (cm min^{-1})	D_L (cm)	SSQ (–)	R^2 (–)
Plot 1 (6 cm)[a]	(0.0389)	(18.30)	1.56 (1.69)	0.989 (0.988)
0–0.33	0.0311	34.61		
0.33–0.58	0.0484	0.03		
0.58–0.71	0.0373	3.65		
0.71–1.25	0.0265	0.02		
Plot 2 (10 cm)	(0.0392)	(17.0)	2.29 (4.22)	2.29 (4.22)
0–0.33	0.0290	17.39		
0.33–0.58	0.0711	0.40		
0.58–0.71	0.0635	37.76		
0.71–1.25	0.0547	49.20		
Plot 3 (14 cm)	(0.0497)	(12.50)	5.11 (6.32)	0.984 (0.984)
0–0.33	0.0380	15.11		
0.33–0.58	0.0736	0.93		
0.58–0.71	0.0709	3.25		
0.71–1.25	0.0560	0.50		
Plot 4 (6 cm)	(0.0436)	(8.30)	0.984 (0.984)	0.996 (0.995)
0–0.33	0.0231	13.90		
0.33–0.58	0.0889	7.67		
0.58–0.71	0.0612	32.73		
0.71–1.25	0.0754	0.35		
Plot 5 (10 cm)	(0.0996)	(2.60)	3.10 (3.50)	0.990 (0.988)
0–0.33	0.0397	5.73		
0.33–0.58	0.0835	9.57		
0.58–0.71	0.0635	24.69		
0.71–1.25	0.0392	13.91		
CV (%)	36.1 (47.5)	102.5 (55.1)		

[a] Water level in the furrow.

Table 3. Summary of the optimized soil hydraulic (n and θ_s) and solute transport (D_L) parameters for the different soil horizons and experimental plots obtained using the two–step optimization method. Values of SSQ and R^2 after estimating D_L (the second step of the analyses) are given in parentheses.

Depth (m)	n (–)	θ_s (cm^3 cm^{-3})	D_L (cm)	SSQ (–)	R^2 (–)
Plot 1 (6 cm)[a]				1.12 (0.444)	0.988 (0.610)
0–0.33	1.56	0.300	34.52		
0.33–0.58	1.56	0.320	0.03		
0.58–0.71	1.75	0.383	3.95		
0.71–1.25	1.92	0.430	2.26		
Plot 2 (10 cm)				0.645 (0.511)	0.987 (0.579)
0–0.33	1.72	0.300	15.54		
0.33–0.58	1.73	0.430	0.06		
0.58–0.71	1.96	0.300	34.37		
0.71–1.25	1.56	0.300	26.60		
Plot 3 (14 cm)				0.927 (0.583)	0.984 (0.47)
0–0.33	1.80	0.368	15.49		
0.33–0.58	1.66	0.300	0.32		
0.58–0.71	1.94	0.300	0.55		
0.71–1.25	2.35	0.340	62.14		
Plot 4 (6 cm)				0.85 (0.466)	0.996 (0.566)
0–0.33	1.50	0.330	10.14		
0.33–0.58	1.57	0.300	1.95		
0.58–0.71	1.51	0.300	6.12		
0.71–1.25	1.53	0.306	0.15		
Plot 5 (10 cm)				0.847 (0.191)	0.991 (0.835)
0–0.33	1.56	0.304	2.62		
0.33–0.58	1.56	0.341	35.10		
0.58–0.71	1.56	0.352	100.00		
0.71–1.25	1.56	0.368	62.20		
CV (%)	12.6	12.8	131.7		

[a] Water level in the furrow.

Much of the differences in the optimized K_s values for the homogeneous and heterogeneous (layered) soil profiles were due to differences in the VG parameters (α and n in particular) caused by scaling of the soil water retention data. Despite the relatively large differences in estimated K_s values, SSQ values of the objective function (table 2) did not significantly decrease (except for plot 4 and somewhat for plot 2). This was mostly because of the low sensitivity of the soil water contents to K_s (fig. 2a).

The optimized D_L values (table 2) varied with depth, most likely because of variability in other soil properties. The D_L values differed significantly from one horizon/plot to another, ranging from 0.02 to 49.20 cm. This somewhat erratic behavior is similar to results obtained from our analyses assuming homogeneous profiles (Abbasi et al., 2003b), for other experimental columns (e.g., Mallants et al., 1994, 1996b), and for many other field–scale studies (e.g., Forrer et al., 1999; Jacques, 2000). The erratic behavior of D_L in field studies appears to be related to spatial variability in the soil water content and the presence presumably of more irregular flow patterns. Unlike results for the homogeneous profiles, the estimated D_L values did not show a noticeable dependency on either the water level or the water/solute application time (except for the first soil horizon). This suggests that variability in the soil physical and chemical properties played a more important role than the imposed flow conditions. The D_L values for the first horizon showed some dependency on the water level and the water/solute application time. The SD experiments produced larger D_L values as compared with the SWS experiments, which agrees with results for the equivalent homogeneous soil profiles.

Two–Step Optimization

Two–step, sequential estimations of the soil hydraulic and solute transport parameters were carried out in an attempt to further improve our model predictions. During the first step, the most sensitive parameters (θ_s and n) were optimized for the different soil horizons, while during the second step, only D_L values were estimated. Two–step optimization results are summarized in table 3. Note that SSQ and R^2 for the estimated D_L values during the second step are given in parentheses. The two–step method produced much lower SSQ values (table 3) compared to simultaneous estimation of the K_s and D_L parameters (table 2). This is an immediate consequence of using classical sequential estimation for the soil hydraulic parameters followed by estimation of the solute transport parameters. However, regressions between measured and predicted solute concentrations were still relatively low, generally between 0.47 and 0.84 for the different plots (table 3). Optimized values for n varied between 1.50 and 2.35, with a CV of 12.6%, while θ_s ranged from 0.30 to 0.43 cm^3 cm^{-3}, with a CV of 12.8%. Both parameters exhibited relatively low variability with depth and among the plots (except n in plot 3 and θ_s in plot 1). The obtained θ_s values overall were lower than those measured in the laboratory (table 1). This is consistent with the fact that field–measured θ_s values are generally much lower than the porosity because of entrapped air (e.g., Klute, 1986).

Contrary to the θ_s and n parameters, D_L varied considerably with depth and between plots, ranging from 0.03 to 100.0 cm, with an overall CV of 131.7%. However, the values were fairly similar, particularly for the first soil horizon, to those estimated simultaneously with K_s and to those obtained assuming homogeneous soil profiles (table 2). Estimated D_L values were also comparable with those previously obtained at the same field site by Bowman and Rice (1986) under intermittent basin irrigation conditions (semi–weekly water application). Their dispersivity values, fitted to a one–dimensional CDE, ranged between 20.8 and 141.0 cm. The higher CV of the estimated D_L values, as compared to that obtained during simultaneous estimation of K_s and D_L, was likely related to differences in the estimated n and θ_s parameters between the two optimization methods. Note that during the two–step optimization process, K_s values were set equal to those previously estimated assuming homogeneous soil profiles (table 2). Optimization using the K_s values obtained using the simultaneous method produced somewhat higher SSQ values (results not shown here).

Model Predictions

Measured infiltrated data, water contents, and solute concentrations from all five experimental plots are compared with predicted values in figure 3. The calculated values were obtained with the final optimized parameters estimated using the simultaneous and the two–step optimization methods. Two–step optimization generally produced higher R^2 values, especially for the soil water contents. However, the agreement was still relatively poor, probably because of temporal and spatial variability in the soil hydraulic and solute transport properties.

Cumulative Infiltration Rates

Measured and calibrated cumulative infiltration rates for the different optimization scenarios and experiments involving two irrigations are compared in figure 4. Overall, model predictions using the two–step optimization method were satisfactory for the first irrigation (fig. 4a), whereas the simultaneous method considerably underestimated infiltrated water in several cases (plots 4 and 5 in particular). Infiltration rates during the second irrigation were slightly overestimated (fig. 4b), which reflects temporal variability in the soil hydraulic properties from one irrigation to the next. We believe that this was caused by some deterioration of the physical structure of the soil surface during initial wetting, and perhaps by some soil erosion (detachment) and deposition during the irrigations. Note that the simultaneous optimization method resulted in better predictions during the second irrigation (fig. 4b). Model predictions for the homogeneous soil profiles and the two–step methods were more or less the same, partly because the same K_s values were used in the two optimizations.

Water Contents and Bromide Concentrations

Comparisons between measured and calibrated soil water contents and bromide concentrations at various depths, experimental plots, and times (6 hours after the first irrigation and 10 days after the second irrigation for the soil water contents, representing wet and dry conditions, respectively; and 5 days after the first irrigation and 20 days after the second irrigation for solute concentrations) are presented in figures 5 and 6, respectively. Experimental plots 1, 3, and 5

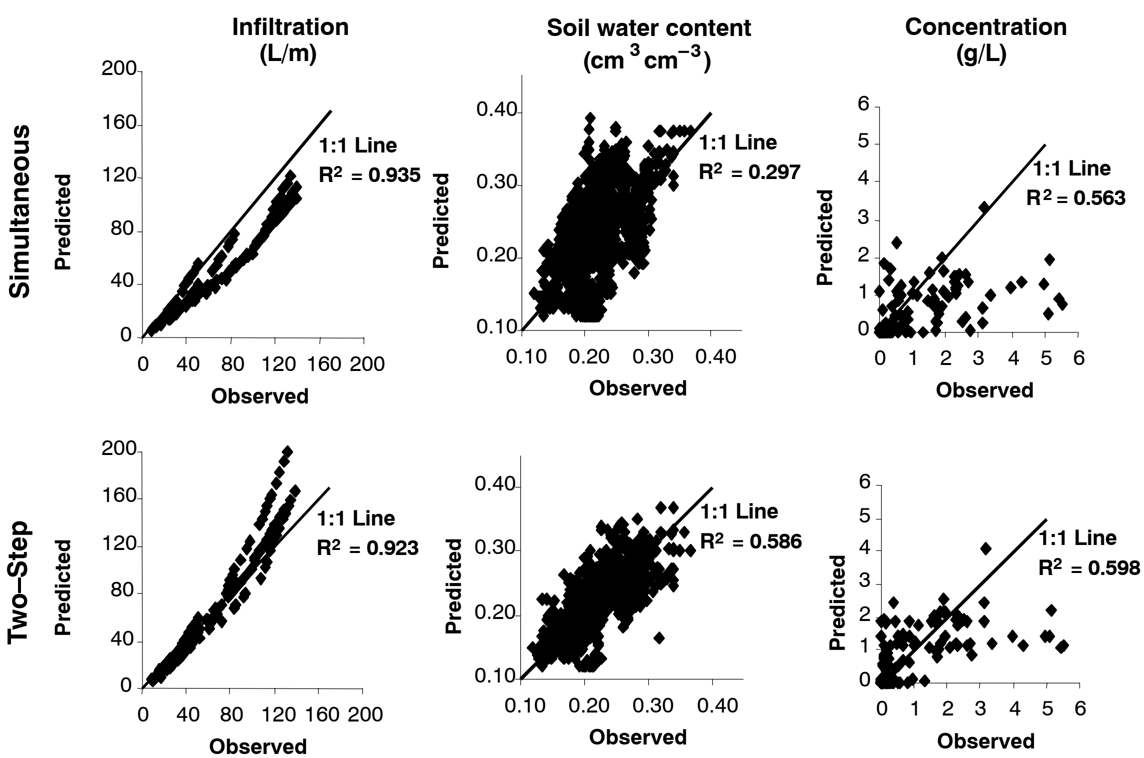

Figure 3. Measured versus predicted (using simultaneous and two–step parameter estimation) cumulative infiltration rates, soil water contents, and solute concentrations for five experimental plots.

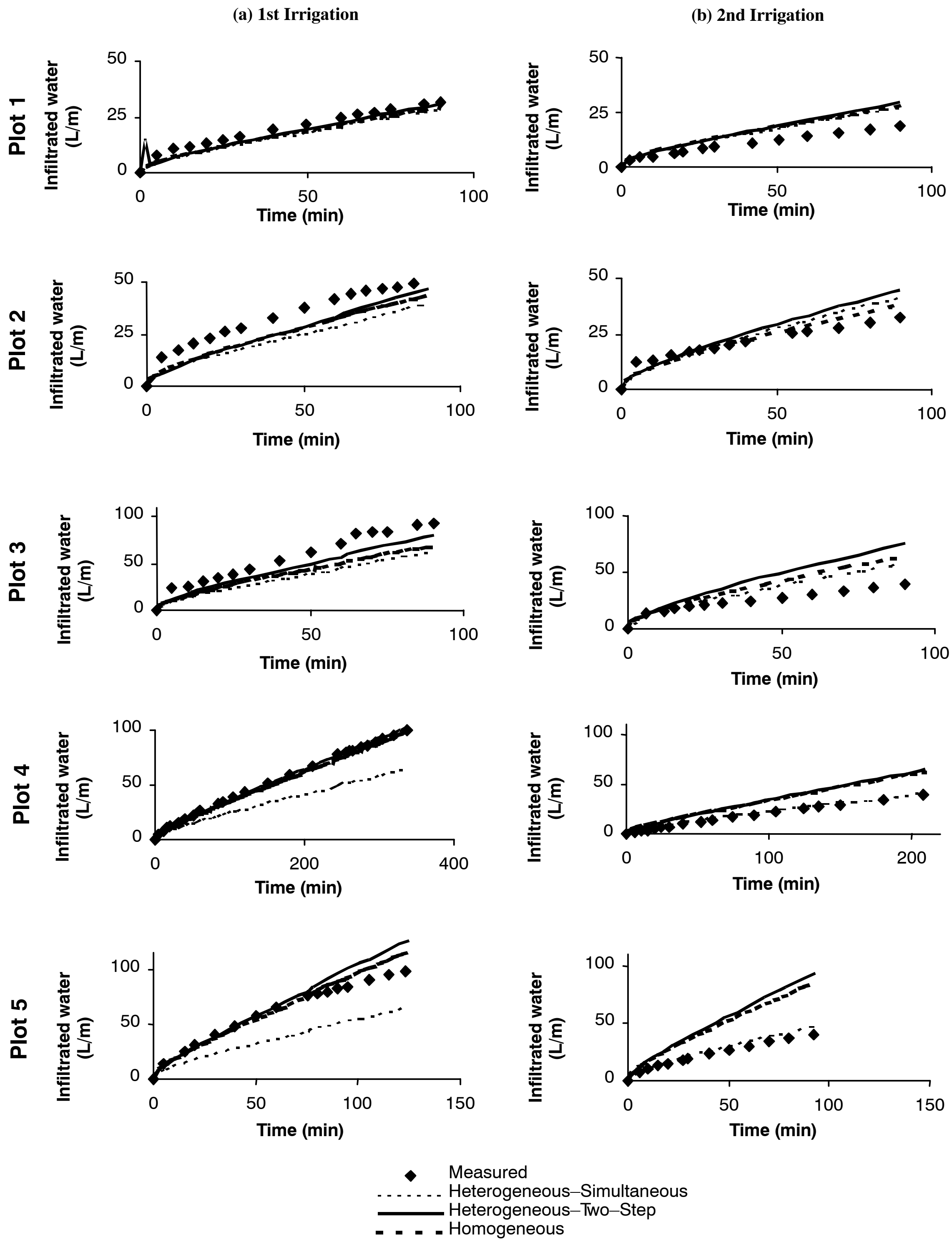

Figure 4. Measured and calibrated cumulative infiltration rates (using different calibration methods) for the different plots during two irrigation events: (a) first irrigation, and (b) second irrigations.

were selected for the comparisons since they were the most representative of the SD experiments, the transient experiment between the SD and SWS experiments, and the SWS experiments, respectively. Results are given by means of one–dimensional curves for better visual comparison between measured data and model predictions. Agreement between the observed and simulated results was relatively poor during wet conditions 6 hours after the first irrigation (fig. 5a). All invoked optimization scenarios overestimated the soil water contents in the soil surface horizons (20 and 40 cm) but provided better predictions at deeper depths. The two–step method considerably improved the predictions for the surface horizons of plots 1 and 5. Agreement during the drier conditions 10 days after the second irrigation (fig. 5b) was somewhat better, but not excellent. The two–step method again produced better predictions, particularly for the surface

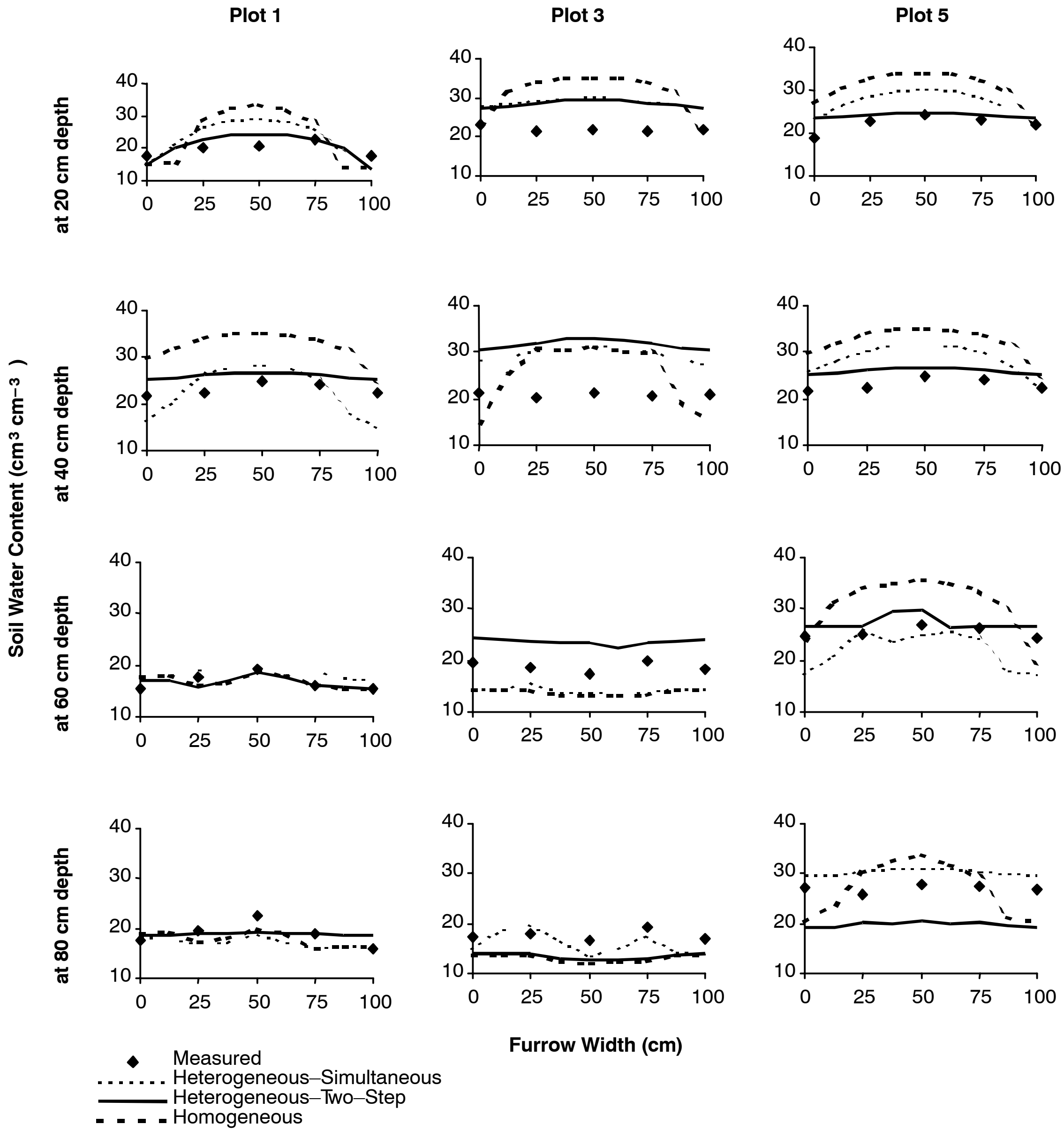

Figure 5a. Measured and calibrated (assuming homogeneous soil profiles, and assuming heterogeneous soil profiles using parameters estimated with simultaneous and two–step calibration) soil water contents for various depths and experimental plots, 6 hours after the first irrigation.

horizon (e.g., 20 cm). Agreement between measured and predicted values obtained using homogeneous soil profiles was less than that obtained using the simultaneous and two–step optimization methods for the heterogeneous profiles.

In spite of the considerable variability and uncertainty in solute transport parameters commonly derived from the field–scale studies, reasonably good agreement was obtained in our study between measured and predicted bromide concentrations (fig. 6). The different optimization methods did not produce good descriptions of the relatively high concentrations observed at a few locations in the soil surface horizons (e.g., 20 cm depth of plot 1 in fig. 6a, and plot 3 in fig. 6b). We believe that this was partly due to overestimation of the soil water contents (fig. 5), thus keeping approximately the same total amounts of solute in the surface layers. Concentrations below depths of 60 cm were not included in figure 6a since the measured and predicted values were both very low. Generally, no obvious differences were found between predictions using the assumptions of profile homogeneity or heterogeneity (for both simultaneous and two–step calibration), except in a few cases where none of them described the solute distributions well (e.g., 60 cm depths of plots 1 and 5 in fig. 6b). Two–step sequential optimization was found to have only a small advantage over the simultaneous approach for the solute concentration as opposed to the water content. In some cases, the two–step method (e.g., the 20 cm and 80 cm depths of plot 5 in fig. 6a) produced better results, while in other cases, the simultaneous approach seems to work better (e.g., the 60 cm depths of plots 3 and 5 in fig. 6a).

Deep Percolation Rates

Measured and predicted rates of deep percolation for water (WDP) and solute (SDP) during the 30–day experimental period are presented in table 4. WDP and SDP are

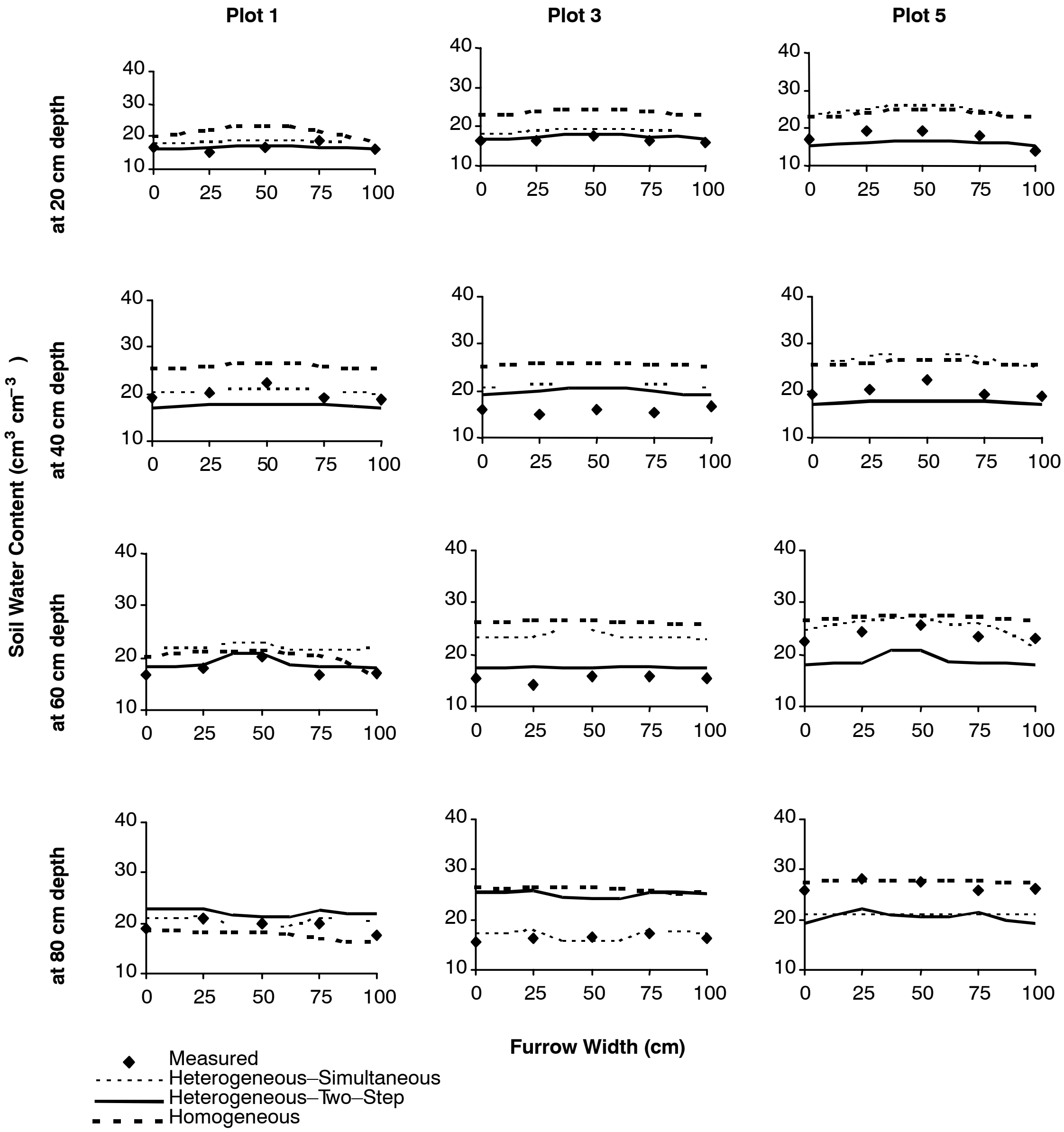

Figure 5b. Measured and calibrated (assuming homogeneous soil profiles, and assuming heterogeneous soil profiles using parameters estimated with simultaneous and two–step calibration) soil water contents for various depths and experimental plots, 10 days after the second irrigation.

defined as the amounts of water and solute, respectively, percolating below a depth of 100 cm. In order to calculate WDP and SDP, soil profiles below the 100 cm depth down to 180 cm were divided into a network of rectangular elements, each being approximately 25 cm by 30 cm. Volumes of water or masses of bromide were determined for each rectangle and then summed to obtain the total amounts of water/bromide. We used daily measured soil water contents of the different depths taken with a neutron probe to estimate the amounts of water, and the measured gravimetric soil water contents, bulk densities, and bromide concentrations of different depths to estimate bromide masses in the soil profiles. Predicted WDP values assuming homogeneous soil profiles were underestimated for the SD plots, and overestimated for plot 5, but provided a reasonable value for plot 4 (table 4). The simultaneous approach generally produced better WDP predictions as compared to the two–step optimization method. However, estimated values were still somewhat underestimated. The two–step method considerably overestimated WDP for all experiments, except for plot 1. The relatively large estimated K_s values of the deeper horizons obtained with the simultaneous optimization method (table 2) did not lead to overestimated WDP values, mostly because of low sensitivity of the soil water contents to the K_s values. The homogeneity assumption and the two–step method gave relatively better predictions of the SDP values (except for plot 5), although SDP was generally underestimated using simultaneous optimization. This in turn was largely due to underestimation of WDP, since convective solute transport is directly related to water flow.

Conclusions

Several soil hydraulic parameters and longitudinal dispersivities were inversely estimated from five different transient experiments on blocked–end furrows assuming the presence

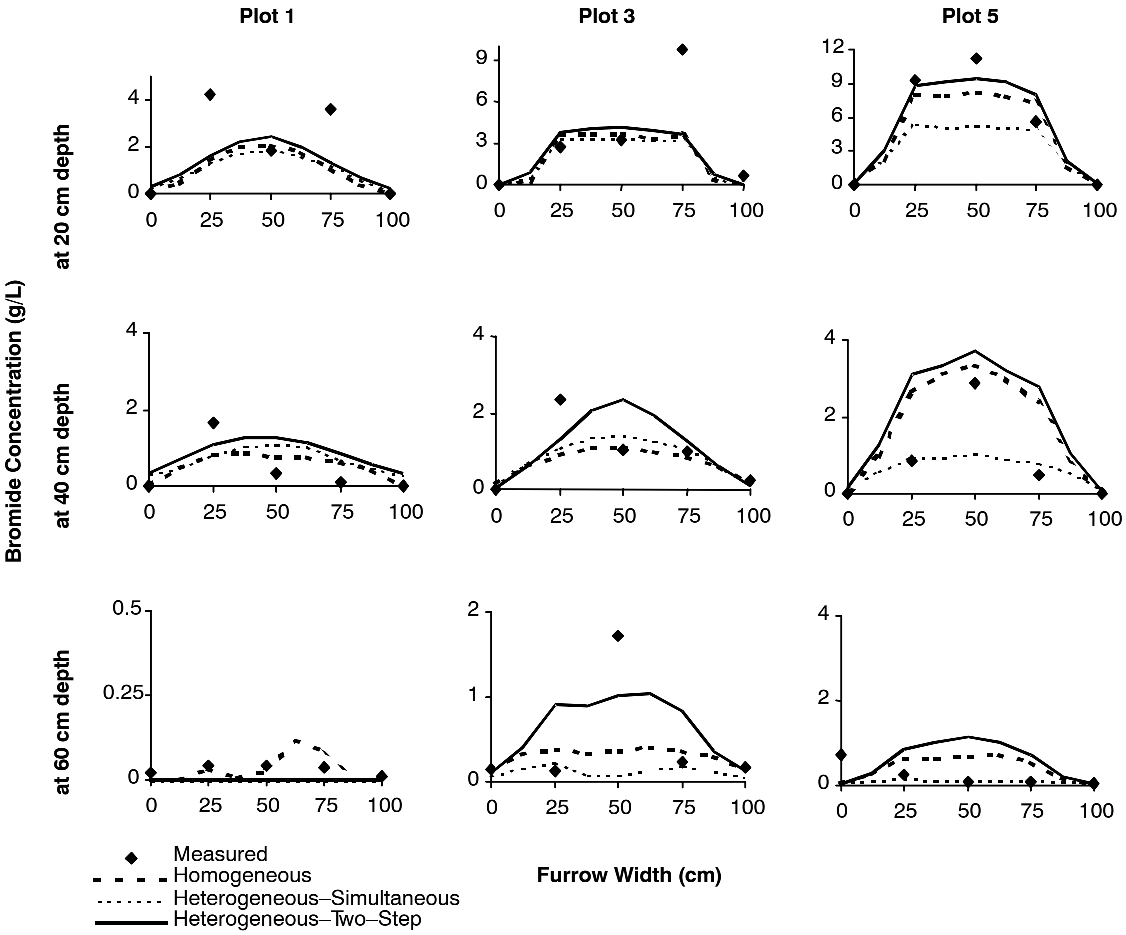

Figure 6a. Measured and calibrated (assuming homogeneous soil profiles, and assuming heterogeneous soil profiles using parameters estimated with simultaneous and two–step calibration) bromide concentrations for various depths and experimental plots, 5 days after the first irrigation.

of four soil horizons. First, the saturated hydraulic conductivity and the longitudinal dispersivities were simultaneously estimated for the different soil horizons and compared with those previously obtained from the same experiments using the assumption of profile homogeneity. Results showed only minor improvements in the model predictions. To improve the predictions, the most sensitive unknown soil hydraulic and solute transport parameters were estimated in two steps by means of sequential estimation of the soil hydraulic parameters followed by the estimation of the transport parameters. This two–step method somewhat improved the predicted cumulative infiltration rate during the first irrigation event, and more significantly the soil water contents, particularly of the surface horizons, while predictions of the deep percolation rates of water did not improve. The different parameter estimation techniques predicted the solute concentrations in the soil profiles reasonably well, considering the temporal and spatial variability in the soil hydraulic and solute transport properties, without obvious differences between the various optimization approaches.

In spite of implementing a scaling procedure for the unsaturated soil hydraulic properties, variability in the optimized longitudinal dispersivity values for the layered soil profiles was found to be higher than for the homogeneous ones. This increased variability was associated with variations in the scaled soil water retention curves of the different soil horizons.

The longitudinal dispersivity of the upper soil horizons showed some dependency on the water level in the furrows and the water/solute application time; similar dependencies were not apparent for the other horizons. An important advantage of scaling was to decrease the computational times by a factor of about 5. Considering temporal variability in the soil hydraulic parameters between the first and second irrigations, presumably because of physical deterioration of the furrow surfaces, could have further improved the model predictions.

In this study, we did not consider hysteresis in the local soil water retention functions. Including hysteresis likely would produce slightly better predictions. However, Kaluarachchi and Parker (1987) and Lenhard et al. (1991) showed that neglecting hysteresis had only relatively little effect on the results in their studies. We felt that our measured data were insufficient to provide an accurate description of hysteresis. Predictions probably could also be improved by using dual–porosity and/or dual–permeability models for water flow and/or solute transport (Simunek et al., 2001). However, models of this type require many more input parameters, and consequently many more measurements, that generally are not available or are difficult to obtain for field–scale experiments.

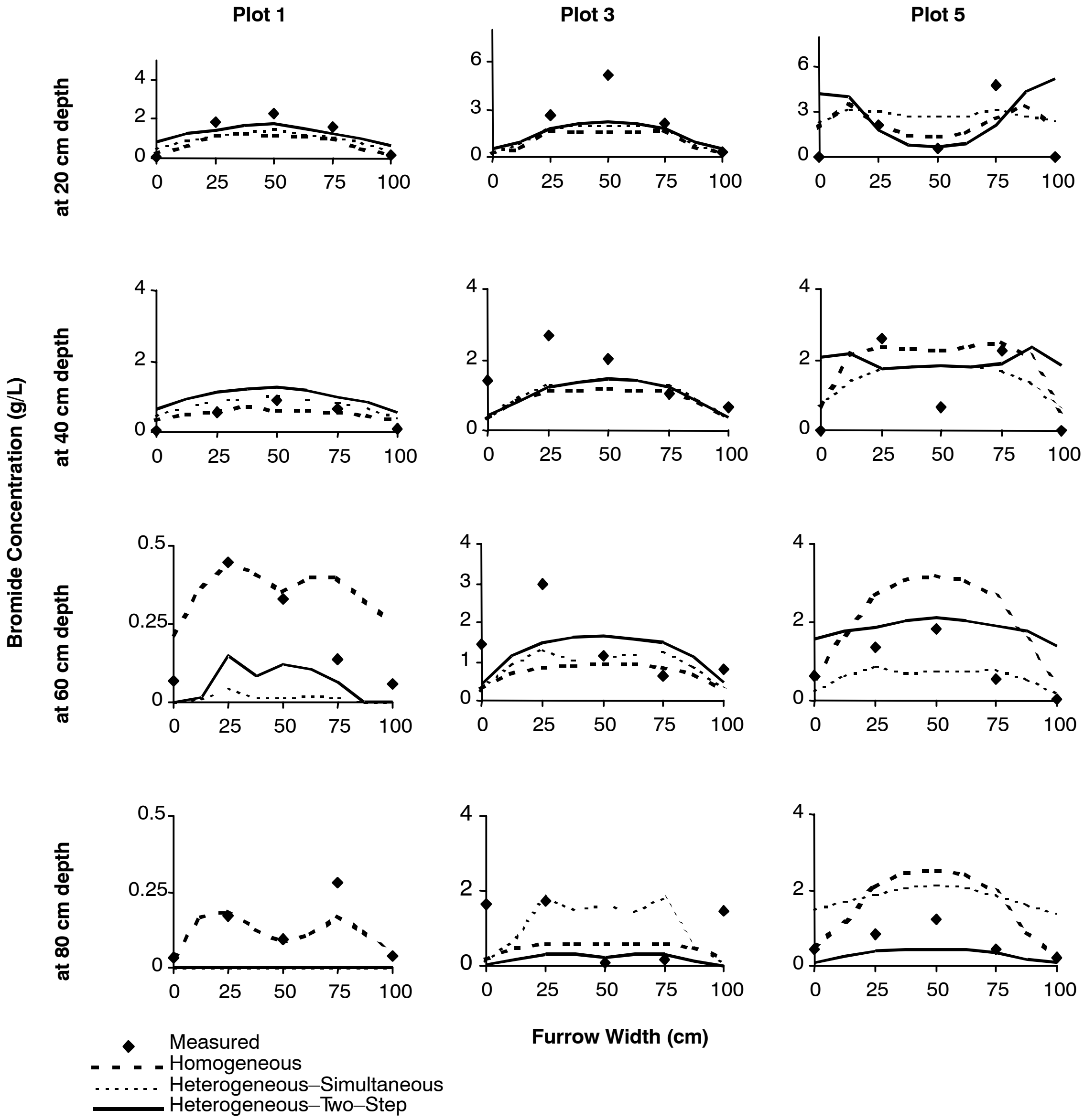

Figure 6b. Measured and calibrated (assuming homogeneous soil profiles, and assuming heterogeneous soil profiles using parameters estimated with simultaneous and two–step calibration) bromide concentrations for various depths and experimental plots, 20 days after the second irrigation.

Table 4. Measured and predicted deep percolation rates for water and solute at the different experimental plots using various optimization approaches.

	Water (L/m)				Solute (g/m)			
		Predicted				Predicted		
Experiment	Measured	Homogeneous Soil Profile	Simultaneous Method	Two–Step Method	Measured	Homogeneous Soil Profile	Simultaneous Method	Two–Step Method
SD[a]								
Plot 1 (6 cm)[b]	11.4	0.0	11.9	8.5	1.1	0.0	0.0	0.0
Plot 2 (10 cm)	16.5	0.0	0.4	29.7	2.9	0.0	0.0	1.7
Plot 3 (14 cm)	29.2	5.9	11.5	88.7	3.5	1.8	0.0	26.5
SWS[c]								
Plot 4 (6 cm)	37.5	30.4	16.3	88.8	27.2	13.0	0.3	18.5
Plot 5 (10 cm)	39.5	118.4	27.3	166.4	15.9	41.0	3.0	169.1

[a] SD = same duration experiments.
[b] Water level in furrow.
[c] SWS = same amount of applied water and bromide experiments.

Acknowledgements

This study was partially supported by SAHRA (Sustainability of Semi–Arid Hydrology and Riparian Areas) under the STC Program of the National Science Foundation, Agreement No. EAR–9876800.

References

Abbasi, F., F. J. Adamsen, D. J. Hunsaker, J. Feyen, P. Shouse, and M. Th. van Genuchten. 2003a. Effects of flow depth on water flow and solute transport in furrow irrigation: Field data analysis. *J. Irrig. and Drainage Eng*. 129(4): 237–246.

Abbasi, F., J. Simunek, J. Feyen M. Th. van Genuchten, and P. J. Shouse. 2003b. Simultaneous inverse estimation of soil hydraulic and solute transport parameters from transient field experiments: Homogeneous soil. *Trans. ASAE* 46(4): 1085–1095.

Bowman, R. S., and R. C. Rice. 1986. Transport of conservative tracers in the field under intermittent flood irrigation. *Water Resources Research* 22(11): 1531–1536.

Butters, G. L., and W. A. Jury. 1989. Field–scale transport of bromide in an unsaturated soil: 2. Dispersion modeling. *Water Resources Research* 25(7): 1583–1589.

Carsel, R. F., and R. S. Parrish. 1988. Developing joint probability distributions of soil water retention characteristics. *Water Resources Research* 24(5): 755–769.

de Vos, J. A. 1997. Water flow and nutrient transport in a layered silt loam soil. PhD diss. Wageningen, The Netherlands: Wageningen Agricultural University.

Eching, S. O., J. W. Hopmans, and W. W. Wallender. 1994. Estimation of in situ unsaturated soil hydraulic functions from scaled cumulative drainage data. *Water Resources Research* 30(8): 2387–2394.

Flury, M., H. Fluhler, W. A. Jury, and J. Leuenberger. 1994. Susceptibility of soils to preferential flow of water: A field study. *Water Resources Research* 30(7): 1945–1954.

Forrer, I., R. Kasteel, M. Flury, and H. Fluhler. 1999. Longitudinal and lateral dispersion in an unsaturated field soil. *Water Resources Research* 35(10): 3049–3060.

Ghodrati, M., and W. A. Jury. 1990. A field study using dyes to characterize preferential flow of water. *SSSA J*. 54(6): 1558–1563.

Gribb, M. M. 1996. Parameter estimation for determining hydraulic properties of a fine sand from transient flow measurements. *Water Resources Research* 32(7): 1965–1974.

Hopmans, J. W., 1989. Stochastic description of field–measured infiltration data. *Trans. ASAE* 32(6): 1987–1993.

Inoue, M., J. Simunek, S. Shiozawa, and J. W. Hopmans. 2000. Simultaneous estimation of soil hydraulic and solute transport parameters from transient infiltration experiments. *Advances in Water Resources* 23(7): 677–688.

Jacques, D. 2000. Analysis of water flow and solute transport at the field scale. PhD diss. No. 454. Leuven, Belgium: Katholieke Universiteit Leuven, Fac. Landbouwkundige en Toegepaste Biologische Wetenschappen.

Jacques, D., D. J. Kim, J. Diels, J. Vanderborght, H. Vereecken, and J. Feyen. 1998. Analysis of steady–state chloride transport through two heterogeneous field soils. *Water Resources Research* 34(10): 2539–2550.

Jacques, D., J. Simunek, A. Timmerman, and J. Feyen. 2002. Calibration of Richards' and convection–dispersion equations to field–scale water flow and solute transport under rainfall conditions. *J. Hydrology* 259: 15–31.

Jaynes, D. B., R. S. Bowman, and R. C. Rice. 1988. Transport of a conservative tracer in the field under continuous flood irrigation. *SSSA J*. 52(3): 618–624.

Kaluarachchi, J. J., and J. C. Parker. 1987. Effects of hysteresis with air entrapment on water flow in the unsaturated zone. *Water Resources Research* 23(10): 1967–1976.

Klute, A. 1986. Water retention: Laboratory methods. A. Klute, ed. *Methods of Soil Analysis: Part 1. Physical and Mineralogical Methods*, 2nd ed. *Agronomy* 9(1): 635–662. Madison, Wisc.: American Society of Agronomy.

Kodesova, R., M. M. Gribb, and J. Simunek. 1998. Estimating soil hydraulic properties from transient cone permeameter data. *Soil Science* 163(6): 436–453.

Kodesova, R., S. E. Ordway, M. M. Gribb, and J. Simunek. 1999. Estimating of soil hydraulic properties with cone permeameter: Field studies. *Soil Science* 164(8): 527–541.

Lenhard, R. J., J. C. Parker, and J. Kaluarachchi. 1991. Comparing simulated and experimental hystertic two–phase transient fluid flow phenomena. *Water Resources Research* 27(8): 2113–2124.

Mallants, D., M. Vanclooster, M. Meddahi, and J. Feyen. 1994. Estimating solute transport in undisturbed soil columns using time–domain reflectometry. *J. Contaminant Hydrology* 17(2): 91–109.

Mallants, D., B. P. Mohanty, D. Jacques, and J. Feyen. 1996a. Spatial variability of hydraulic properties in a multi–layered soil profile. *Soil Science* 161(3): 167–181.

Mallants, D., M. Vanclooster, and J. Feyen. 1996b. Transect study on solute transport in a macroporous soil. *Hydrological Processes* 10(1): 55–70.

Marquardt, D. W. 1963. An algorithm for least squares estimation of non–linear parameters. *J. Ind. Appl. Math*. 11: 431–441.

Mualem, Y. 1976. A new model for predicting the hydraulic conductivity of unsaturated porous media. *Water Resources Research* 12(3): 513–522.

Richards, L. A. 1931. Capillary conduction of liquids through porous medium. *Physics* 1: 318–333.

Roth, K., W. A. Jury, H. Fluhler, and W. Attinger. 1991. Transport of chloride through an unsaturated field soil. *Water Resources Research* 27(10): 2533–2541.

Russo, D., J. Zaidel, and A. Laufer. 1994a. Stochastic analysis of solute transport in partially saturated heterogeneous soil: I. Numerical experiments. *Water Resources Research* 30(3): 769–779.

Russo, D., J. Zaidel, and A. Laufer. 1994b. Stochastic analysis of solute transport in partially saturated heterogeneous soil: II. Prediction of solute spreading and breakthrough. *Water Resources Research* 30(3): 781–790.

Schaap, M. G., and F. J. Leij. 1998. Database related accuracy and uncertainty of pedotransfer functions. *Soil Science* 163(10): 765–779.

Simmons, C. S., D. R. Nielsen, and J. W. Biggar. 1979. Scaling of field–measured soil water properties. *Hilgardia* 47: 77–154.

Simunek, J., and M. Th. van Genuchten. 1996. Estimating unsaturated soil hydraulic properties from tension disc infiltrometer data by numerical inversion. *Water Resources Research* 32(9): 2683–2696.

Simunek, J., and M. Th. van Genuchten. 1997. Estimating unsaturated soil hydraulic properties from multiple tension disc infiltrometer data. *Soil Science* 162(6): 383–398.

Simunek, J., O. Wendroth, and M. Th. van Genuchten. 1998. Parameter estimation analysis of the evaporation method for determining soil hydraulic properties. *SSSA J*. 62(4): 894–905.

Simunek J., M. Sejna, and M. Th. van Genuchten. 1999. The HYDRUS–2D software package for simulating the two–dimensional movement of water, heat, and multiple solutes in variably saturated media, Version 2.0. IGWMC–TPS–70. Golden Colo.: Colorado School of Mines, International Ground Water Modeling Center.

Simunek, J., O. Wendroth, N. Wypler, and M. Th. van Genuchten. 2001. Non–equilibrium water flow characterized by means of upward infiltration experiments. *European J. Soil Science* 52(1): 13–24.

Simunek, J., D. Jacques, J. W. Hopmans, M. Inoue, M. Flury, and M. Th. van Genuchten. 2002. Solute transport during variably–saturated flow – Inverse methods. Chapter 6.6 in *Methods of Soil Analysis: Part 1. Physical Methods*, 1435–1449. 3rd ed. J. H. Dane and G. C. Topp, eds. Madison, Wisc.: SSSA.

Snow, V. O., B. E. Clothier, D. R. Scotter, and R. E. White. 1994. Solute transport in a layered field soil: Experiments and modeling using the convection–dispersion approach. *J. Contaminant Hydrology* 16(4): 339–358.

Steenhuis, T. S., and R. E. Muck. 1988. Preferred movement of nonadsorbed chemicals on wet, shallow, sloping soils. *J. Environ. Quality* 17(3): 376–384.

Troiano, J., C. Garretson, C. Krauter, J. Brownell, and J. Hutson. 1993. Influence of amount and method of irrigation water application on leaching of atrazine. *J. Environ. Quality* 22(2): 290–298.

Vanderborght, J., C. Gonzalez, M. Vanclooster, D. Mallants, and J. Feyen. 1997. Effects of soil type and water flux on solute transport. *SSSA J*. 61(2): 372–389.

Vanderborght, J., M. Vanclooster, A. Timmerman, P. Seuntjens, D. Mallants, D.–J. Kim, D. Jacques, L. Hubrechts, C. Gonzalez, J. Feyen, J. Diels, and J. Deckers. 2001. Overview of inert tracer experiments in key Belgian soil types: Relation between transport and soil morphological and hydraulic properties. *Water Resources Research* 37(12): 2873–2888.

van Genuchten, M. Th. 1980. A closed–form equation for predicting the hydraulic conductivity of unsaturated soils. *SSSA J*. 44(5): 892–898.

van Weesenbeeck, I. J., and R. G. Kachanoski. 1994. Effect of variable horizon thickness on solute transport. *SSSA J*. 58(5): 1307–1316.

Ventrella, D., B. P. Mohanty, J. Simunek, N. Losavio, and M. Th. van Genuchten. 2000. Water and chloride transport in a fine–textured soil: Field experiments and modeling. *Soil Science* 165(8): 624–631.

Vogel, T., M. Cislerova, and J. W. Hopmans. 1991. Porous media with linearly variable hydraulic properties. *Water Resources Research* 27(10): 2735–2741.

Vrugt, J. A., M. T. van Wijk, J. W. Hopmans, and J. Simunek. 2001. One–, two–, and three–dimensional root water uptake functions for transient modeling. *Water Resources Research* 37(10): 2457–2470.

Warrick, A. W., G. J. Mullen, and D. R. Nielsen. 1977. Scaling field–measured soil hydraulic properties using a similar media concept. *Water Resources Research* 13(2): 355–362.

White, R. E., J. S. Dyson, Z. Gerstl, and B. Yaron. 1986. Leaching of herbicides through undisturbed cores of a structured clay soil. *SSSA J*. 50(2): 277–283.

Wildenschild, D., J. W. Hopmans, and J. Simunek. 2001. Flow rate dependence of soil hydraulic characteristics. *SSSA J*. 65(1): 35–48.